

Stereocontrol of Intramolecular Diels–Alder Reactions: Synthetic Studies and Transition Structure Modeling with C5-Substituted 1,3,8-Nonatrienes and Nonadienyne

Craig I. Turner,[†] Rachel M. Williamson,[‡] Michael N. Paddon-Row,^{*,§} and Michael S. Sherburn^{*,†}

School of Chemistry, University of Sydney, Sydney, NSW 2006, Australia, School of Chemistry, University of New South Wales, Sydney, NSW 2052, Australia, and Institute of Fundamental Sciences, Massey University, Private Bag 11222, Palmerston North, New Zealand

m.sherburn@chem.usyd.edu.au

Received January 11, 2001

An investigation into the *endo/exo* selectivity and π -diastereofacial selectivity of ester-tethered intramolecular Diels–Alder reactions is reported. High levels of *exo* selectivity are realized with terminally substituted dienophiles, and high *lk* π -diastereofacial selectivities are induced by the presence of a bulky dioxolanyl substituent at the allylic position of the tether. Precursors **19S**, **20S**, and **21S**, readily prepared from glucose, provide densely functionalized bicyclic lactones of predictable stereochemistry in high yields in enantiomerically pure form upon thermolysis at 110 °C. B3LYP/6-31G(d) theory provides good descriptions of transition structures for these reactions and allows an understanding of the formation of the major cycloadducts.

Introduction

The hydroisobenzofuran-1-one moiety **1** is common in natural products, with many such compounds displaying important, in some cases unique, biological activities. For example, himbacine **2** is a potent, selective muscarinic receptor antagonist;¹ triptolide **3** both exhibits potent antitumor activities and inhibits lymphocyte proliferation and interleukin-2 production;² and myrocin C **4** is an antitumor antibiotic (Figure 1).³ This bicyclic lactone has also proven useful as a starting point for the construction of other synthetically challenging natural molecules with elaborate architectures.^{4–6} Enantiocontrolled synthetic routes to compounds containing the hydroisobenzofuran-1-one subunit are, therefore, of significant interest.

An efficient synthetic entry to compounds containing this structural subunit is by way of the intramolecular Diels–Alder (IMDA) reaction.⁷ The influence of dienophile substitution upon the *endo/exo* selectivity of such intramolecular cycloadditions has been the focus of our recent synthetic and computational efforts.⁸ Thus, calculations carried out at the B3LYP/6-31G(d) level of theory correctly predict both the stereoselective formation

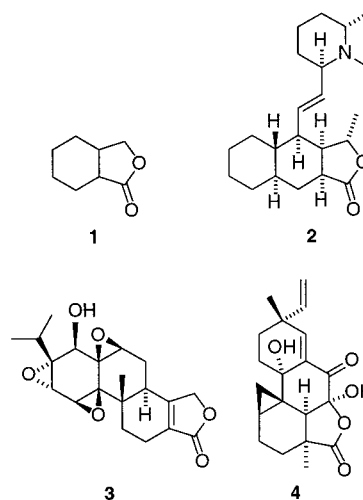


Figure 1. The hydroisobenzofuran-1-one structure **1** and representative natural products containing this subunit.

of *trans*-fused *exo* cycloadducts⁹ in IMDA reactions of *Z*-substituted 1,3,8-nonatriene **5**¹⁰ and a lower *exo/endo* selectivity for the corresponding *E*-substituted precursor **8** (Scheme 1).

[†] University of Sydney.

[§] University of New South Wales.

[‡] Massey University.

(1) (a) Pinhey, J. T.; Ritchie, E.; Taylor, W. C. *Aust. J. Chem.*, **1961**, *14*, 106–134. (b) Chackalamannil, S.; Davies R. J.; Wang, Y.; Asberom, T.; Doller, D.; Wong, J.; Leone, D.; McPhail A. T. *J. Org. Chem.* **1999**, *64*, 1932–1940 and references therein.

(2) Yang, D.; Ye, X.-X.; Xu, M.; Pang, K.-W.; Zou, N.; Letcher, R. M. *J. Org. Chem.* **1998**, *63*, 6446–6447.

(3) (a) Hsu, Y. H.; Hirota, A.; Shoji, S.; Nagakawa, M.; Adachi, T.; Nozaki, H.; Nakayama, M. *J. Antibiot.* **1989**, *42*, 223–224. (b) Chumoy, M. Y.; Danishefsky, S. J.; Schulte, G. C. *J. Am. Chem. Soc.* **1994**, *116*, 11213–11228.

(4) Borzilleri, R. M.; Weinreb, S. M.; Parvez, M. *J. Am. Chem. Soc.* **1995**, *117*, 10905–10913.

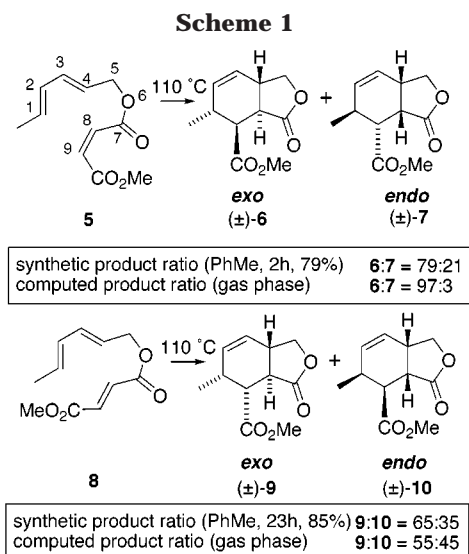
(5) Arseniyadis, S.; Brondi-Alves, R.; Yashunsky, D. V.; Potier, P.; Toupet, L. *Tetrahedron* **1997**, *53*, 1003–1014.

(6) Berthon, L.; Tahri, A.; Uguen, D. *Tetrahedron Lett.* **1994**, *35*, 3937–3940.

(7) Reviews on the IMDA reaction: (a) Taber, D. F. *Intramolecular Diels–Alder and Alder Ene Reactions*; Springer-Verlag: Berlin, 1984. (b) Fallis, A. G. *Can. J. Chem.* **1984**, *62*, 183–234. (c) Ciganek, E. *Org. React.* **1984**, *32*, 1–374. (d) Craig, D. *Chem. Soc. Rev.* **1987**, *1987*, 187–238. (e) Roush, W. R. In *Advances in Cycloaddition*; Curran, D. P., Ed.; JAI: Greenwich, CT, 1990; Vol. 2, pp 91–146. (f) Roush, W. R. In *Comprehensive Organic Synthesis*; Trost, B. M., Fleming, I., Paquette, L. A., Eds.; Pergamon: Oxford, 1991; Vol. 5, pp 513–550. (g) Craig, D. In *Stereoselective Synthesis (Houben-Weyl)*, 4th ed.; Thieme: Stuttgart, 1995; Vol. E 21 c, pp 2872–2904.

(8) Lilly, M. J.; Paddon-Row, M. N.; Sherburn, M. S.; Turner, C. I. *Chem. Commun.* **2000**, 2213–2214.

(9) We use the terms *endo* and *exo* to describe the orientation of the dienophile tether connection with respect to the diene. An *endo* orientation of the dienophile tether affords the *cis*-fused bicycle; an *exo* orientation of the dienophile tether furnishes the *trans*-fused cycloadduct.



All B3LYP/6-31G(d) transition structures (TSs) located exhibited both asymmetric stretch and twist attributes. The developing *internal* (C4–C8) bond in each TS was invariably shorter than the developing *peripheral* (C1–C9) bond. Close analysis of the size and orientation of the twist asymmetry about the developing shorter *internal* bond allowed a rationalization of the experimental results in terms of an extended version of Houk's twist-asynchronicity model.¹¹

In another study, we discovered that the π -*diastereofacial* selectivity of IMDA reactions of this type can be controlled by the influence of substituents about a stereocenter at the diene terminus (Scheme 2).¹² In this case, high-level theoretical models indicate that subtle conformational preferences dictate to which face of the diene the dienophile will dock.¹³

We felt that a contemporaneous study with substrates bearing a stereocenter at the allylic position of the tether (i.e., at C5 rather than the diene terminus C1¹³) might provide further insights into both the *exo/endo* and π -*diastereofacial* preferences of this IMDA reaction, thereby facilitating its synthetic application. Very recently, White and Snyder¹⁴ disclosed their preliminary findings on experimental and computational aspects of the IMDA reaction of acrylate **14** (Scheme 3), a key step in their elegant synthetic approach toward pillaromycinone.¹⁵ Thus, upon heating to 250 °C in a sealed vessel, a solution of rhamnose-derived acrylate **14** provided a mixture of three of the four possible stereoisomeric cycloadducts **15**–**18**. Transition structures leading to the four IMDA adducts were located using the MM2* procedure,^{11b} and single point energies for these TSs were calculated at the B3LYP/6-31G(d) level (e.g., B3LYP/6-

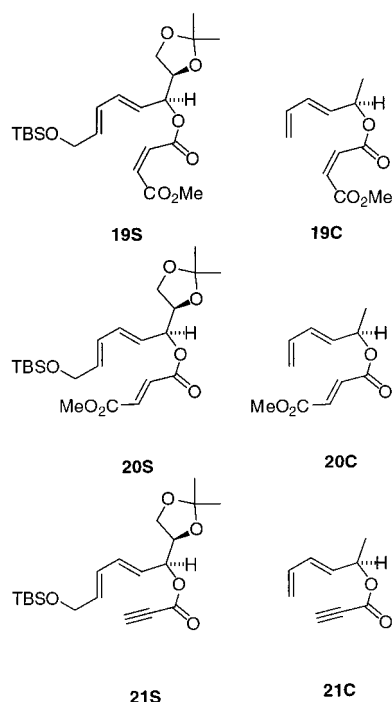
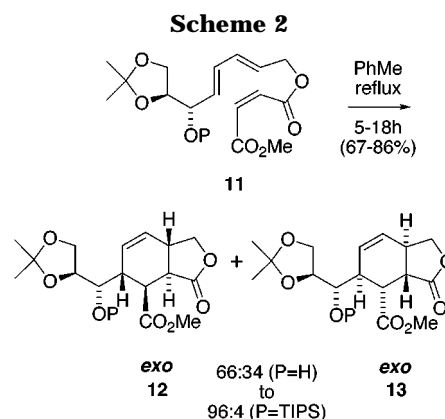


Figure 2. The three IMDA precursors prepared and thermolyzed **19S**, **20S**, and **21S**, and their theoretical counterparts **19C**, **20C**, and **21C**, under scrutiny by DFT.



31G(d)//MM2*). Interestingly, the MM2*-optimized TSs for IMDA reaction of **14** exhibit a longer developing *internal* bond and shorter developing *peripheral* bond,¹⁴ the reverse of that found by us in *fully optimized* B3LYP/6-31G(d) TSs for related IMDA reactions.^{8,13} This difference in developing bond lengths notwithstanding, the combined B3LYP/6-31G*//MM2* method correctly identifies *endo*, *lk*¹⁶ adduct **15** as the major product.

The appearance of the White–Snyder study¹⁴ prompts us to report our own synthetic and computational investigations with tether-induced stereocontrol in IMDA reactions. Thus, continuing our focus on the development of methods for the prediction and control of both *exo/endo* selectivity and π -*diastereofacial* selectivity, we have examined IMDA reactions of C9-substituted, glucose-derived trienes **19S** and **20S** (Figure 2). In addition, to gauge the level of π -*diastereofacial* selectivity in this system “cleanly” (i.e., without the added complication of *exo/endo* selectivity) we have prepared and cyclized propynoate precursor **21S**. These synthetic results are complemented by the calculation of the TSs for IMDA reactions of structures **19C**, **20C**, and **21C** which have

(10) For ease of comparison between the all-carbon prototype and esters described here, 1,3,8-nonatriene numbering is retained throughout.

(11) (a) Brown, F. K.; Singh, U. C.; Kollman, P. A.; Raimondi, L.; Houk, K. N.; Bock, C. W. *J. Org. Chem.* **1992**, *57*, 4862–4869. (b) Raimondi, L.; Brown, F. K.; Gonzalez, J.; Houk, K. N. *J. Am. Chem. Soc.* **1992**, *114*, 4796–4804. (c) Brown, F. K.; Houk, K. N. *Tetrahedron Lett.* **1985**, *26*, 2297–2300.

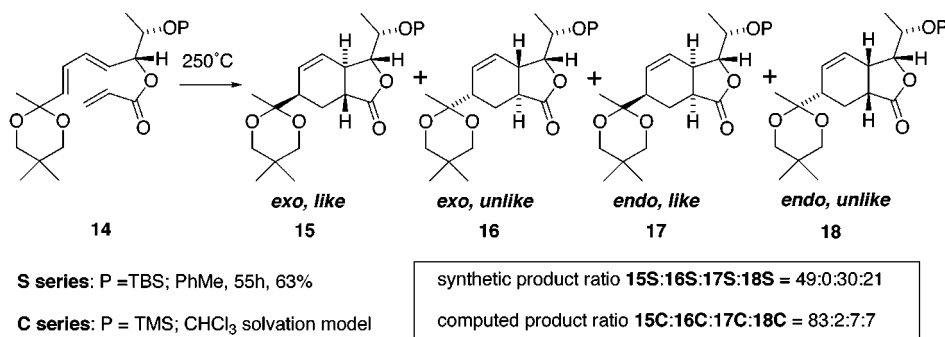
(12) Lilly, M. J.; Sherburn, M. S. *Chem. Commun.* **1997**, 967–968.

(13) Paddon-Row, M. N.; Sherburn, M. S. *Chem. Commun.* **2000**, 2215–2216.

(14) White, J. D.; Demnitz, F. W. J.; Oda, H.; Hassler, C.; Snyder, J. P. *Org. Lett.* **2000**, *2*, 3313–3316.

(15) White, J. D.; Nolen, E. G., Jr.; Miller, C. H. *J. Org. Chem.* **1986**, *51*, 1150–1152.

Scheme 3

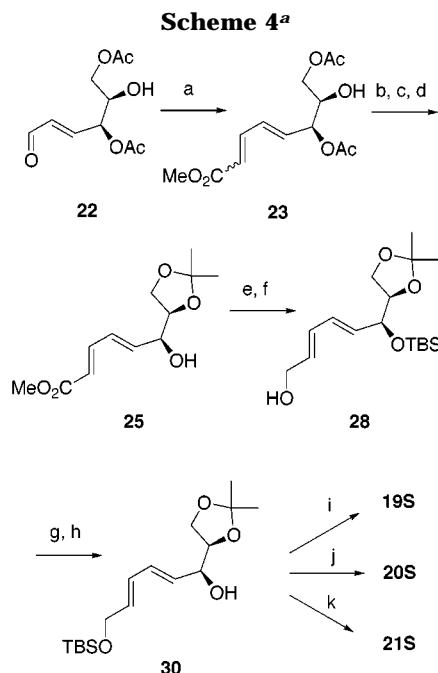


been fully optimized at the B3LYP/6-31G(d) level of theory and their subsequent interpretation.

We were also drawn to these substrates since previous studies have shown that maleate, fumarate, and propionate esters of 2,4-pentadien-1-ols require less forcing conditions for IMDA reactions than do the corresponding acrylates.^{5,6,12,17,19} Indeed, the successful IMDA reaction of acrylate **14** (Scheme 3) is something of an exception, since several other attempts to carry out IMDA reactions of pentadienyl acrylates have been unsuccessful.^{18–24} Whereas some workers have been discouraged from investigating the intramolecular cycloaddition chemistry of these ester-linked 1,3,8-nonatrienes on account of their propensity for polymerization,¹⁸ others have noted a reluctance to cyclize.^{19–24} A major obstacle to cyclization appears to be an equilibrium disfavoring the necessary *s-cis* conformation of the ester linkage,^{7,25} although imaginative methods have been developed to solve this problem.²⁶

Results and Discussion

Synthesis of the three IMDA precursors **19S**, **20S**, and **21S** from readily available, glucose-derived chiral hexenal **22**²⁷ is depicted in Scheme 4. Thus, 4(*S*),6(*R*)-diacetoxy-5-hydroxy-2(*E*)-hexenal **22** was subjected to a Wittig



^a Reagents and conditions: (a) Ph₃P=CHCO₂Me (1.05 equiv), Et₂O, rt, 4 h, 80%; (b) KHCO₃, H₂O–MeOH, rt, 4.5 h, 61%; (c) Me₂C(OMe)₂ (8 equiv), CSA (0.1 equiv), Me₂C=O, 0 °C, 3 h; (d) PhSH (2 × 0.1 equiv), AIBN (2 × 0.05 equiv), PhH, *hν*, 2 h 48% over two steps; (e) imidazole (3.5 equiv), TBSCl (1.7 equiv), DMF, rt, 3.5 h, 98%; (f) DIBAL (2.9 equiv), Et₂O, –70 °C, 0.25 h; (g) TBAF (2.0 equiv), THF, rt, 0.25 h, 87% over two steps; (h) imidazole (2.5 equiv), TBSCl (1.2 equiv), DMF, rt, Ar, 1 h, 99%; (i) Et₃N (1.6 equiv), maleic anhydride (2.2 equiv), DMAP (0.1 equiv), CH₂Cl₂, rt, 2 h then CH₂N₂, Et₂O, 72%; (j) (*E*)-MeO₂CCH=CHCO₂H (1.2 equiv), DCC (1.3 equiv), DMAP (0.1 equiv), CH₂Cl₂, rt, 1 h, 88%; (k) HCCO₂H (4.2 equiv), DCC (4.6 equiv), DMAP (0.3 equiv), CH₂Cl₂, rt, 18 h, 57%.

reaction with Ph₃P=CHCO₂Me to give a 3:1 mixture of the *E,E*- and *E,Z*-diene esters **23**. Mild hydrolysis of the acetates of **23** with potassium hydrogen carbonate produced the triol. Formation of the desired monosubstituted dioxolane derivative from the triol was accompanied by significant quantities of the regioisomeric disubstituted compound (ratio of primary alcohol:secondary alcohol = 59:41). This mixture of regioisomers and geometrical isomers was equilibrated to the *E,E*-dienes by exposure to thiyl radicals, from which the desired compound **25** was isolated by chromatography. Multigram quantities of **25** were prepared routinely in this way.²⁸ The hydroxy ester **25** could not be reduced directly to the correspond-

(28) In principle, the unwanted regioisomeric dioxolane could be recycled by employing a deprotection–reprotection cycle.

(16) We use the Seebach–Prelog descriptor *like* (*lk*) to describe a cycloadduct resulting from the approach of the dienophile to the *re* face of the diene with an allylic stereocenter of *R* configuration. The term *unlike* (*ul*) refers to *si/R* and *re/S* combinations, see: Seebach, D.; Prelog, V. *Angew. Chem., Int. Ed. Engl.* **1982**, *21*, 654–660. For consistent use of this convention, the priorities of the groups about the allylic stereocenter are assigned such that the sp² carbon has a higher priority than the sp³ carbon: Tripathy, R.; Franck, R. W.; Onan, K. D. *J. Am. Chem. Soc.* **1988**, *110*, 3257–3262. Adam, W.; Glaser, J.; Peters, K.; Prein, M. *J. Am. Chem. Soc.* **1995**, *117*, 9190–9193.

(17) White, J. D.; Sheldon, B. G. *J. Org. Chem.* **1981**, *46*, 2273–2280.

(18) House, H. O.; Cronin, T. H. *J. Org. Chem.* **1965**, *30*, 1061–1070.

(19) Birtwhistle, D. H.; Brown, J. M.; Foxton, M. W. *Tetrahedron* **1988**, *44*, 7309–7318.

(20) Toyota, M.; Wada, Y.; Fukumoto, K. *Heterocycles* **1993**, *35*, 111–114.

(21) Strekowski, L.; Kong, S.; Battiste, M. A. *J. Org. Chem.* **1988**, *53*, 901–904.

(22) Hecker, S. J.; Heathcock, C. H. *J. Org. Chem.* **1985**, *50*, 5159–5166.

(23) Fraser-Reid, B.; Benko, Z.; Guiliano, R.; Sun, K. M.; Taylor, N. *J. Chem. Soc., Chem. Commun.* **1984**, 1029–1030.

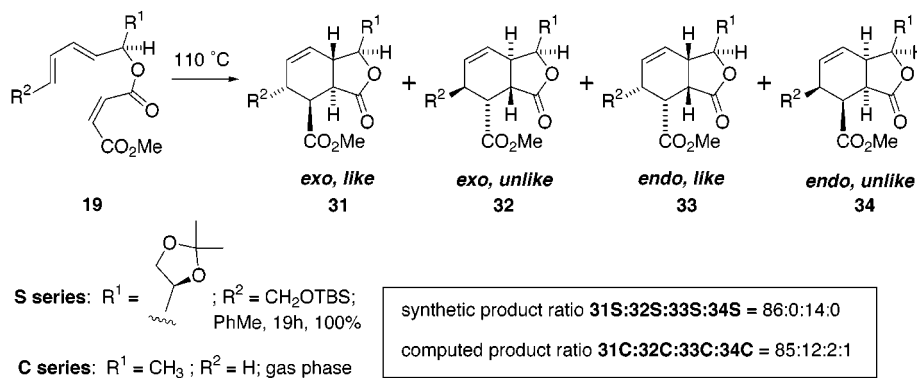
(24) Burke, S. D.; Smith Strickland, S. M.; Powner, T. H. *J. Org. Chem.* **1983**, *48*, 454–459.

(25) For a seminal study on the rate-retarding influence of ester tethers upon IMDA reactions, see: Boeckman, R. K., Jr.; Demko, D. M. *J. Org. Chem.* **1982**, *47*, 1789–1792.

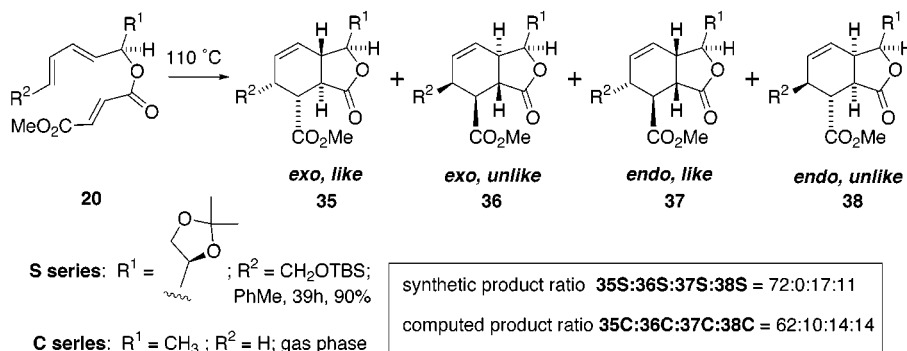
(26) (a) Jung, M. E. *Synlett* **1990**, 186–190. (b) Jung, M. E. *Synlett* **1999**, 843–846 and references therein.

(27) Perlin, A. S.; Gonzalez, F.; Lesage, S. *Carbohydr. Res.* **1975**, *42*, 267–274.

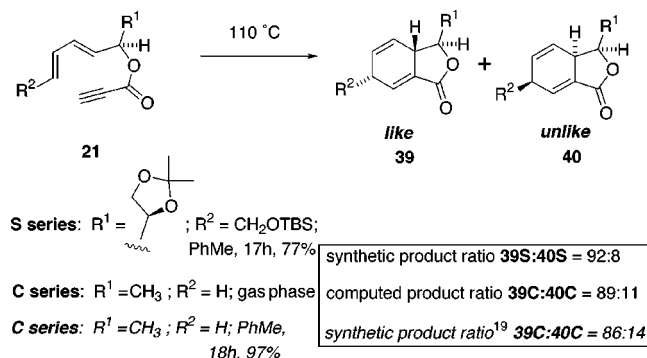
Scheme 5



Scheme 6



Scheme 7



ing diol, so the alcohol was first protected as the *tert*-butyldimethylsilyl ether prior to DIBAL reduction. Deprotection of the silyl ether of the secondary allylic alcohol **28** with TBAF followed by selective protection of the primary allylic alcohol provided the desired dienol **30** in high yield.

Dienol **30** was readily converted into the three IMDA precursors. Reaction of **30** with maleic anhydride afforded the maleate half ester as an unstable oil which was converted immediately to the more stable *Z*-methyl ester **19S** by methylation with ethereal diazomethane. (*E*)-Methyl ester **20S** and propynoate **21S** were obtained by esterification of the dienol with methyl hydrogen fumarate and propynoic acid, respectively.

Intramolecular Diels–Alder reactions of these three substrates were carried out in dilute solutions in refluxing toluene in the presence of a small amount of anti-oxidant (Schemes 5–7). The maleate derivative **19S** gave a very clean conversion into two (of the possible four) cycloadducts in quantitative yield, which were easily separated by column chromatography (Scheme 5).

Thermolysis of the fumarate ester **20S** at 110 °C required roughly twice the reaction time of the maleate ester **19S** to proceed to completion. Once again, a clean reaction ensued (90% isolated yield) and three chromatographically separable cycloadducts were obtained (Scheme 6).²⁹

Thermolysis of the propynoate ester **21S** at 110 °C was both fast and once again highly stereoselective, providing a mixture of the two possible cycloadducts which were, in our hands, not separable (Scheme 7).

COSY and NOESY experiments allowed the elucidation of the full stereostructures of all seven products.³⁰ The *trans*-ring fusion of the *exo* adducts **31S** and **35S** was clearly evident from a large 1,2-*trans*-diaxial coupling constant (13.0–13.5 Hz) between the protons attached to the ring junction carbons. The *endo* adducts **33S**, **37S**, and **38S** exhibited a smaller (8.2–10.8 Hz) coupling constant between the same protons, indicating *cis*-ring fusion.

To ascertain whether these product ratios are the result of a kinetically or thermodynamically controlled reactions, pure cycloadducts from the maleate and fumarate reactions were re-subjected to the same reaction conditions used to bring about their intramolecular cycloaddition. No change was observed in each case, indicating that these reactions are, as expected, subject to kinetic control.

The observed stereoselectivities from the IMDA reactions described above were investigated by carrying out density functional calculations (DFT), at the B3LYP/6-

(29) For related synthetic studies with racemic precursors carrying *E*-dienophiles, see refs 5, 6, and 19. While the proportions of the minor products differ, in each case the *exo*, *lk* cycloadduct predominates.

(30) Pertinent NOE's are listed in the Experimental Section.

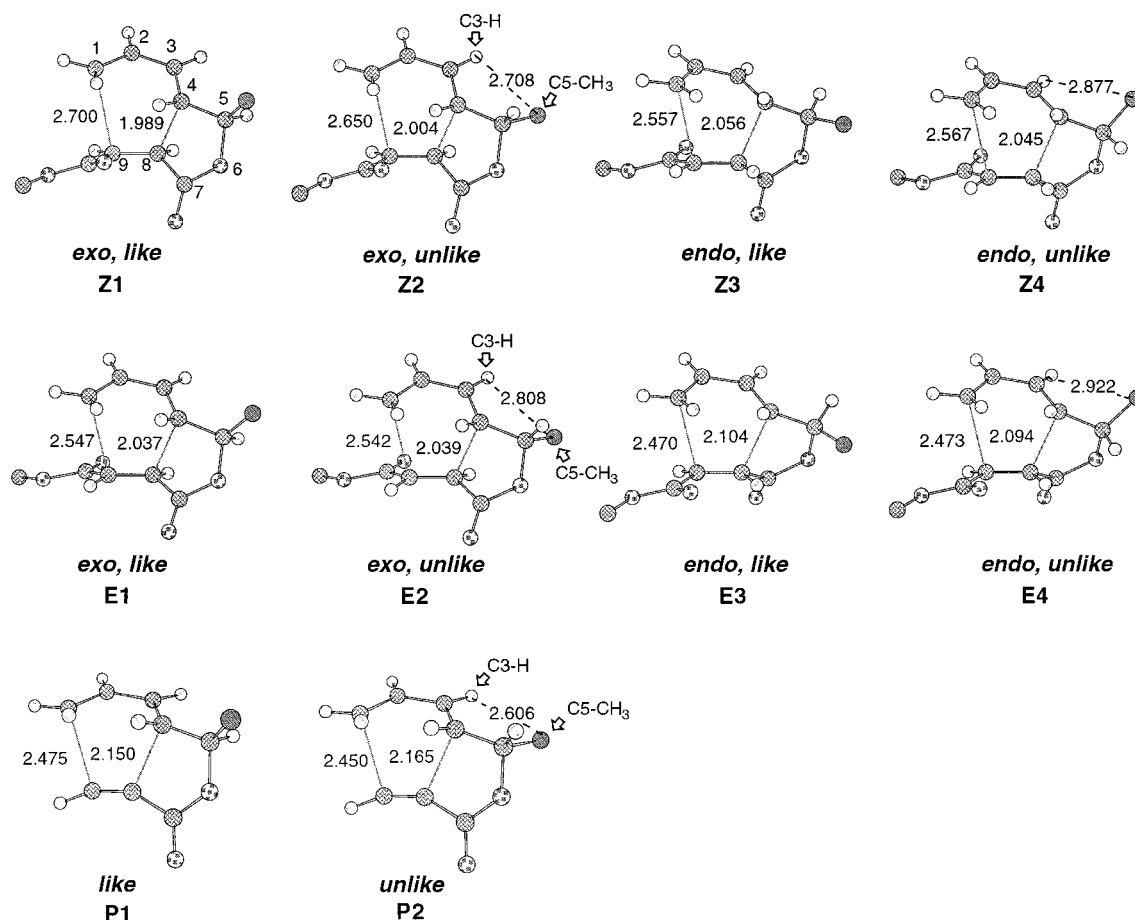


Figure 3. IMDA TS geometries for **19C** (**Z1–Z4**), **20C** (**E1–E4**), and **21C** (**P1–P2**). For ease of comparison, the enantiomeric structure is depicted in the *ul* series. Distances shown are in angstroms. Hydrogens are omitted from the C5 methyl groups (darkened) for clarity.

31G(d) level,³¹ on model transition structures of these reactions. It has been demonstrated that this level of theory gives reliable energetic and structural data for transition structures for both intermolecular and intramolecular Diels–Alder reactions.^{8,13,32,33} Due to the size of precursors **19S**, **20S**, and **21S** and their accompanying conformational flexibility, prototypes **19C**, **20C**, and **21C** were employed. Initially, we were somewhat apprehensive about the level of accuracy in TS modeling which might result from removing the C1-substituent and most of the C5-dioxalanyl group from **19S**, **20S**, and **21S**. Earlier work has shown, however, that a change from C1-H to C1-CH₃ in this system has a negligible effect on the *endo* and *exo* TS geometries and their relative energies.⁸ We are confident, therefore, that with even greater differences between the synthetic and computational series, the calculations would still capture the essential features driving the stereoselectivities in the experimental systems and that we would witness a close correlation between the ratios of the four possible products.

All transition structures were fully optimized at the B3LYP/6-31G(d) level, using the GAUSSIAN 98 set of programs,³⁴ and they were characterized by harmonic vibrational frequency calculations. The product distributions reported in Schemes 5, 6, and 7 were calculated from Boltzmann distributions at 383 K using electronic energies of the TSs, corrected for zero point energies. Drawings of the TSs, together with selected geometric data, are displayed in Figure 3. Full structural details (Z-matrices) and energies of all TSs are provided in the Supporting Information.

Scheme 5 presents comparative data for IMDA reactions of synthetic and computational *Z*-dienophile systems **19S** and **19C**. Corresponding data for the *E*-dienophile series and the propynoate series are listed in Scheme 6 and Scheme 7, respectively. In each case, the relative proportions of products from the synthetic process are listed alongside predicted Boltzmann distribu-

(31) (a) Becke, A. D. *J. Chem. Phys.* **1993**, *98*, 5648. (b) Lee, C.; Yang, W.; Parr, R. G. *Phys. Rev. B* **1988**, *37*, 785. For reviews of density-functional methods, see: (c) Ziegler, T. *Chem. Rev.* **1991**, *91*, 651. (d) *Density Functional Methods in Chemistry*; Labanowski, J., Andzelm, J., Eds.; Springer: Berlin, 1991. (e) Parr, R. G.; Yang, W. *Density-Functional Theory of Atoms and Molecules*; Oxford University Press: New York, 1989.

(32) Houk, K. N.; Li, Y.; Evanseck, J. D. *Angew. Chem., Int. Ed. Engl.* **1992**, *31*, 682 and references therein.

(33) Wiest, O.; Houk, K. N. *Top. Curr. Chem.* **1996**, *183*, 1.

(34) Frisch, M. J.; Trucks, G. W.; Schlegel, H. B.; Scuseria, G. E.; Robb, M. A.; Cheeseman, J. R.; Zakrzewski, V. G.; Montgomery, J. A., Jr.; Stratmann, R. E.; Burant, J. C.; Dapprich, S.; Millam, J. M.; Daniels, A. D.; Kudin, K. N.; Strain, M. C.; Farkas, O.; Tomasi, J.; Barone, V.; Cossi, M.; Cammi, R.; Mennucci, B.; Pomelli, C.; Adamo, C.; Clifford, S.; Ochterski, J.; Petersson, G. A.; Ayala, P. Y.; Cui, Q.; Morokuma, K.; Malick, D. K.; Rabuck, A. D.; Raghavachari, K.; Foresman, J. B.; Cioslowski, J.; Ortiz, J. V.; Baboul, A. G.; Stefanov, B. B.; Liu, G.; Liashenko, A.; Piskorz, P.; Komaromi, I.; Gomperts, R.; Martin, R. L.; Fox, D. J.; Keith, T.; Al-Laham, M. A.; Peng, C. Y.; Nanayakkara, A.; Gonzalez, C.; Challacombe, M.; Gill, P. M. W.; Johnson, B.; Chen, W.; Wong, M. W.; Andres, J. L.; Gonzalez, C.; Head-Gordon, M.; Replogle, E. S.; Pople, J. A. *Gaussian 98*, Revision A.7 ed.; Gaussian Inc: Pittsburgh, PA, 1998.

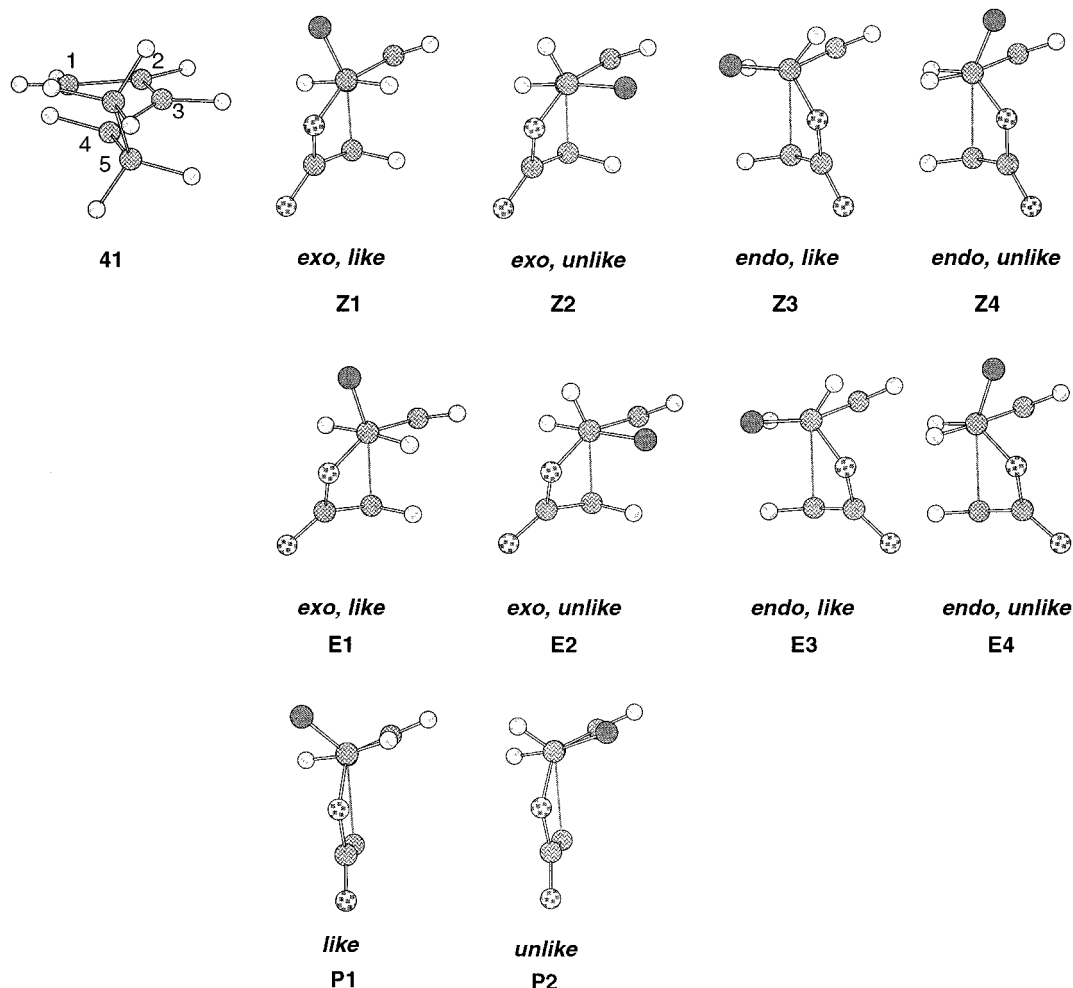


Figure 4. 1,3-Hexadiene **41** and profile views of IMDA TSs **Z1–Z4**, **E1–E4**, and **P1–P2**. The enantiomeric structure is depicted in the *ul* TS series. Hydrogens are omitted from the C5 methyl groups (darkened) in the TSs for clarity.

tions for fully optimized B3LYP/6-31G(d) IMDA TSs.³⁵ In the case of propynoate **39C** (Scheme 7), experimental data for the “model” IMDA reaction is available from work of the Birtwhistle group.¹⁹

The following conclusions can be drawn from the results depicted in Schemes 5–7 and Figures 3–4.

1. *The synthetic and computational results agree in both the nature of the major stereoisomer and its relative abundance.* We conclude from this that structures **19C**, **20C**, and **21C** serve as good models for the synthetic systems **19S**, **20S**, and **21S**. As such, it is probable that features which make TSs **Z1**, **E1**, and **P1** (Figure 3, which lead to the major computed stereoisomers **31C**, **35C**, and **39C** respectively) the most energetically favorable of their respective groupings will also be useful for rationalizing the formation of predominant diastereomers **31S**, **35S**, and **39S**. Furthermore, the reported¹⁹ stereochemical outcome for the IMDA reaction of propynoate ester **39C** agrees very closely with our calculated Boltzmann distribution for this substrate.

2. *Both E- and Z-alkenic dienophiles preferentially form the thermodynamically less stable trans-fused exo cycloadducts, rather than the more stable cis-fused endo*

cycloadducts. According to the Houk twist asynchronicity model,¹¹ recently refined for this system by us,⁸ *exo* products are generally preferred over *endo* products with C9-substituted 1,3,8-nonatrienes since the *exo* TS is able to accommodate a larger degree of stabilizing asymmetric twist. Thus, in the *exo* TS, C9 is twisted about the developing C4–C8 bond in the *exo* (outside)¹¹ direction, whereas the *endo* TS must suffer a more strained asymmetric twisting mode in the *endo* (inside)¹¹ direction. Our refinement of this twist asynchronicity model⁸ highlights the increased strain suffered by *E*-dienophiles in the *exo* TS. These unfavorable interactions account for the lower *exo:endo* ratios witnessed in *E*-dienophile substrates vs their *Z*-dienophile counterparts. In the present study—and in agreement with these previous findings on simpler substrates—both theory and experiment show that the precursor containing a *Z*-dienophile, **19**, once again undergoes a more *exo*-selective IMDA reaction than its *E*-dienophile congener **20**. Furthermore, we note that both the experimentally observed and the calculated *exo* selectivity of C5-substituted trienes (Scheme 5 and Scheme 6) is higher than that seen both with C5-unsubstituted compounds (Scheme 1) and acrylates (Scheme 3). That the presence of a C5-methyl group in our systems leads to a moderate enhancement of the *exo* selectivity may be explained simply in terms of the B3LYP/6-31G(d) conformational energy profile for 1,3-

(35) In each IMDA TS, two discrete orientations of the terminal ester group with respect to the dienophile C=C bond are possible. Both *s-cis* and *s-trans* TSs give similar product ratios.⁸ Data for the slightly lower energy *s-cis* TSs are discussed here.

hexadiene, **41**, about the C4–C5 bond (rigid rotor approximation; the geometry resembles that found in the IMDA TSs). Referring to the profiles of the C5-methyl IMDA TSs, depicted in Figure 4, the conformations of both *endo*, *lk* and *endo*, *ul* TSs (**Z3**, **Z4**, **E3**, and **E4**) about the C4–C5 bond correspond approximately to conformational energy *maxima* for 1,3-hexadiene since both suffer eclipsing interactions between a C5-group and the C4–H bond.³⁶ A similar effect is observed for butene.³⁷ In contrast, the conformations of both *exo*, *lk* and *exo*, *ul* TSs (**Z1**, **Z2**, **E1**, and **E2**) correspond approximately to energy *minima* for 1,3-hexadiene. Thus, the presence of the C5-methyl substituent has the effect of accentuating the *exo/endo* energy difference by way of this additional steric and torsional strain.

3. The predominant stereoisomeric product results from *lk* approach of the dienophile to the diene. π -Diastereofacial selectivity in related systems has been discussed⁷ in terms of a minimization of developing ^{1,3}A strain³⁸ during the intramolecular cycloaddition process. Specifically, dienophile approach to one π -diastereoface of the diene incurs a penalty caused by destabilizing nonbonded eclipsing interactions between the C5 substituent and C3–H. This interaction is clearly visible in TSs **Z2**, **E2**, and **P2** (Figure 3 and Figure 4), which lead to *ul* cycloadducts **32C** (*exo*), **36C** (*exo*), and **40C**, respectively. Such ^{1,3}A strain is present to a much lesser extent in *endo*, *ul* TSs **Z4** and **E4**, as evidenced by longer (C3)H⋯(C5)CH₃ distances. The *endo*, *ul* TSs are further destabilized, however, by the close proximity of C5–H to C4–H (2.353 Å in **Z4** and 2.384 Å in **E4**). The *endo*, *lk*-TSs **Z3** and **E3** are destabilized relative to **Z1** and **E1** due to C5–CH₃ eclipsing C4–H (dihedral angles 1.4° and 1.3°, respectively). Thus, *exo*, *lk* cycloadducts **31** and **35** and *lk* cycloadduct **39** are formed in these reactions since transition states leading to them (modeled by TSs **Z1**, **E1**, and **P1**) lack these destabilizing nonbonded interactions.

In summary, a tether dioxolanyl group invokes a strong *lk* π -diastereofacial preference in IMDA reactions of 1,3,8-nonatrienes and nonadienynes. In the triene series, *exo* mode cycloadditions are dominant over *endo* cycloadditions with both *E*- and *Z*-dienophiles, a result of some significance in light of the lack of *exo/endo* selectivity with dienophiles unsubstituted at C9 (Scheme 3).^{5,6} These

two stereodirecting influences coalesce in triene precursors **19S** and **20S** such that one of four possible products is formed in a synthetically useful quantity in each case. The hexahydroisobenzofuranone cycloadducts thus formed, **31S** and **35S**, are enantiomerically pure and rich in functionality, which should allow further synthetic elaboration at every position of the bicyclic framework.

The level of *exo* selectivity is higher with glucose-derived trienes **19S** and **20S** than the simpler systems **5** and **8** but the origin of this improvement is unclear at this stage.³⁹ In addition, π -diastereofacial selectivities observed in the present glucose-derived system are slightly higher than those reported previously^{14,15} (cf. Schemes 5–7 vs Scheme 3). This marginal improvement may be due either to the dioxolanyl substituent operating as a slightly more sterically bulky stereodirecting group (by way of ^{1,3}A strain, Figure 3) or simply as a result of the milder reaction conditions (110 vs 250 °C). While differences in the predicted/observed quantities of minor stereoisomers exist, theory and experiment are in agreement with both the identity of the major product and its relative abundance. Thus, DFT-based TS modeling is a powerful predictive tool for increasingly complex IMDA reactions, processes whose stereochemical outcomes are notoriously difficult to predict.⁷ While we can rationalize the formation of the major product in these IMDA reactions, the subtle differences in product distribution among the minor isomers are more difficult to reconcile. Future work from our laboratories will address issues such as this.

Acknowledgment. The authors thank Dr. Pat Edwards (Massey University) and Dr. Ian Luck (University of Sydney) for assistance with NMR experiments, The Australian Research Council for the award of a Senior Research Fellowship (to M.N.P.-R.) and a project grant (to M.S.S.), and the New South Wales Centre for Parallel Computing for allocation of CPU time (to M.N.P.-R.).

Supporting Information Available: Experimental procedures, product characterization data, ¹H NMR spectra of all cycloadducts (**31S**, **33S**, **35S**, **37S**, **38S**, **39S/40S**), energies and final optimized coordinates for stationary points of all transition structures (**Z1**–**Z4**, **E1**–**E4**, and **P1**–**P2**). This material is available free of charge via the Internet at <http://pubs.acs.org>.

JO015516V

(36) ^{1,3}A strain is also responsible for the conformational energy maxima of 1,3-hexadiene. As such, the factors responsible for enhanced *exo/endo* selectivity in IMDA reactions of **19** and **20** (point 2) are necessarily linked with the factors responsible for *lk* selectivity (point 3).

(37) Eliel, E. L.; Wilen, S. *Stereochemistry of Organic Compounds*; Wiley-Interscience: New York, 1994; pp 616–617.

(38) Hoffmann, R. W. *Chem. Rev.*, **1989**, *89*, 1841–1860.

(39) The two structural differences between **19S/20S** and **5/8**, viz., the silyloxymethyl group at C1 and the dioxolanyl group at C5, may both be the cause of improved *exo* selectivity, since the former is present in **11** (which gives *exo* adducts exclusively) and the latter is modeled in **19C/20C** (which predicts an improved *exo* selectivity for these substrates over the corresponding C5-desmethyl analogues⁸).